Original Article

DEVELOPMENT AND EVALUATION OF ORAL SUSTAINED-RELEASE RANITIDINE DELIVERY SYSTEM BASED ON BACTERIAL NANOCELLULOSE MATERIAL PRODUCED BY *KOMAGATAEIBACTER XYLINUS*

THANH XUAN NGUYEN[1*], MUNG VAN PHAM[2], CUONG BA CAO[1]

¹Institute of Scientific Research and Applications, Hanoi Pedagogical University 2, ²Hai Duong Central College of Pharmacy, Vietnam
Email: nguyenxuanthanh@hpu2.edu.vn

ABSTRACT

Objective: The short biological half-life (2-3 h) and low bioavailability (50 %) of ranitidine (RAN) following oral administration favor the development of a controlled release system. This study was aimed to develop and *in vitro* evaluate oral sustained-release RAN delivery system based on the bacterial nanocellulose material (BNM) produced by *Komagataeibacter xylinus* (*K. xylinus*) from selected culture media.

Methods: BNMs are biosynthesized by *K. xylinus* in the standard medium (SM) and coconut water (CW). RAN was loaded in BNMs by the absorption method. The structural and physicochemical properties of BNMs and BNMs-RAN were evaluated via swelling behavior, FTIR, and FESEM techniques. Moreover, the effect of BNMs on RAN release profile and release kinetics was analyzed and evaluated.

Results: The amount of loaded RAN or entrapment efficacy for BNM-CW is higher than for BNM-SM. The BNM-SM-RAN and BNM-CW-RAN exhibited a decreased initial burst release system followed by a prolonged RAN release up to 24 h in relation to the commercial tablets containing RAN. The RAN release from these formulations was found higher in the SGF medium than that of in SIF medium. RAN released from these formulations was found to follow the Korsmeyer-Peppas model and diffusion sustained drug release mechanism. The sustained release of RAN from BNM-SM-RAN was slower than for RAN from BNM-CW-RAN, but the mechanism of sustained RAN release was the same.

Conclusion: Oral sustained-release RAN delivery system based on BNMs was successfully prepared and evaluated for various *in vitro* parameters. The biopolymers like BNM-SM and BNM-CW could be utilized to develop oral sustained RAN release dosage form.

Keywords: Bacterial nanocellulose material (BNM), *Komagataeibacter xylinus* (*K. xylinus*), Oral sustained-release, Ranitidine delivery system

INTRODUCTION

Bacterial nanocellulose material (BNM), a three-dimensional (3D) weblike nanofibrous network structure of cellulose, synthesized in a biotechnological process by *Komagataeibacter xylinus (K. xylinus)* is a biodegradable polymer that recently increased considerable interest in the biopharmaceutical field, as a result of its unique material characteristics, such as extremely high porosity, high purity, high mechanical strength, high nanofibers with an ultrafine network, high water holding capacity, low toxicity, and biocompatibility. Because of its superior properties make it a suitable innovative biofabricated material for serving as a potential candidate in drug delivery system and also as an excipient [1]. Since its nanosized 3D porous networks, including an extremely fine cellulose fiber and nanofibrils of 2-4 nm diameter, BNM is expected to hold large amounts of active ingredients, resulting in an enormous surface area to volume ratio [2]. BNM has already been utilized to develop effective drug delivery systems for different drugs or active molecules, namely serum albumin [3], berberine [4], octenidine [5], polihexanide and povidone-iodine [6], salbutamol [7], famotidine and tizanidine [8], curcumin [9], and phenolic [10], with the benefit of having a structure of nano-cellulose 3D-networks, thus supporting an extended-release of drugs. BNM was used as a delivery system for serum albumin [3]. This research showed that freeze-dried formulations demonstrated a lower uptake capacity for serum albumin than never-dried BNM, which could be explicated by changes in the nanofiber network in the time of the freeze-drying process.

Moreover, the biological activity and integrity of serum albumin could be retained at the time of the loading and release processes. Researchers applied BNM as a carrier for delivery of berberine to prolong drug release time as compared to commercial products and have potential applications in both oral or transdermal drug delivery systems [4]. It was demonstrated that BNM is a potential choice to functionalities with the antiseptic drug octenidine. Octenidine

loaded BNM demonstrated that release profiles were comparable to already marketed products. It was investigated that the octenidine loaded BNM exhibit a tremendous potential as wound dressing with controlled drug delivery [5]. Moreover, BNM was also functionalized with the antiseptics povidone-iodine (PI) and polihexanide (PHMB). PI-loaded BNM showed a delayed-release compared to PHMB due to a high molar drug mass and structural changes induced by PI insertion into BNM that also increased the compressive strength of BNM samples [6]. The other research confirmed that BNM is a promising choice to gelatin capsules with both fast and slow-release properties of the drug depending upon the constitutions of the enclosed materials [7]. The researchers claimed that BNM can be used as a matrix for loading with model drugs (tizanidine is a highly water-soluble drug, famotidine is poorly water-soluble) and assessed as a single excipient based drug delivery system [8].

Ranitidine (RAN) is N-[2-[[[5-[(dimethylamino) methyl]-2-furanyl] methyl]thio]ethyl]-N-methyl-2-nitro-1,1-ethenediamine. RAN is an antisecretory drug with H_2 antagonist action useful in treating gastric and duodenal disorders [11-20]. The adult oral dosage, frequency of RAN is 150 mg twice per d or 300 mg once per d. A conventional dose of 150 mg can inhibit gastric acid secretion up to 5 h but not up to 10 h. An alternative dose of 300 mg leads to plasma fluctuations [18, 20, 21]. The reason for multiple dosing frequencies or high dose is due to its short biological half-life (2-3 h) and low bioavailability (50 %) [13, 15, 18, 21]. In order to overcome these problems, an attempt was made to develop oral sustained-release drug delivery systems for RAN. *In vitro* drug release studies of RAN microspheres showed a controlled release of 11 h with Eudragit RL-100 [11]. The data obtained in this study thus suggest that a microparticulate floating dosage form of an anti-ulcer drug can be successfully designed to give controlled RAN delivery and improved oral bioavailability. Floating *in situ* gel of RAN using natural polymers like sodium alginate and pectin and calcium carbonate as a cross-linking agent was formulated and evaluated [13]. It was shown that the sustained release of RAN can be achieved by *in situ* gel along with good floating properties. RAN buccal films of *Sterculia foetida*

gum in combination with carbopol 934P have shown very good physical stability, excellent mucoadhesive strength, good stability and prolonged drug release [14]. Tripolyphosphate (TPP)-crosslinked chitosan (CH)/poly (ethylene oxide) (PEO) electrospun nanofibrous mats as a floating gastro-retentive delivery system for RAN were prepared and evaluated [19]. Based on the obtained results in this study, TPP-crosslinked CH/PEO nanofibrous mats lower initial burst release and it was showing a prolonged release profile for the RAN from the TPP-crosslinked CH/PEO-RAN electrospun nanofibrous mats. The aim of the present work was to develop and evaluate oral sustained-release RAN delivery system based on BNM produced by *K. xylinus* in selected culture media.

MATERIALS AND METHODS

Materials

The bacterial strain of *Komagataeibacter xylinus* (ATCC 23767) was purchased from the Biological Resource Center, National Institute of Technology and Evaluation, Japan.

Ranitidine 99.5% and yeast extract were purchased from Sigma-Aldrich (USA). Peptone was purchased from ECHA (European Union) and other chemicals used in the analysis were purchased from China. Commercial tablets containing RAN (TAB-RAN) were purchased from the local market. All the analytical grade chemicals and solvents were used as received without additional refinement and analysis.

Methods

Biosynthesis of bacterial nanocellulose material

Bacterial nanocellulose material (BNM) was produced by *Komagataeibacter xylinus* (*K. xylinus*) (ATCC 23767) using the method of static culture in two selected liquid media [3-10, 23] which were composed of the standard medium (SM) and coconut water (CW). Firstly, glucose (20 g), peptone (5 g), diammonium phosphate (2.7 g), yeast extract (5 g), citric acid (1.15 g) and double-distilled water (1000 ml) were used in SM. Secondly, glucose (20 g), peptone (10 g), diammonium phosphate (0.5 g), ammonium sulfate (0.5 g) and coconut water (1000 ml) were used in CW. The selected culture media were sterilized at 121 °C for 20 min.

For pre-culture, *K. xylinus* (ATCC 23767) powder was activated in a 100-ml flask containing 50 ml of pre-culture medium such as glucose (100 g), agar (15 g), CaCO$_3$ (20 g), yeast extract (10 g) and distilled water (1000 ml), initial pH of 6.8. It was incubated at 150 rpm shaking and 28 °C for 2 d using an orbital shaker (Lab companion, SKF-2075, Korea). The activated bacteria were then cultured for 2 d in a 250-ml shaker bottle containing 100 ml SM medium to increase the number of bacteria. After that the pre-culture (10 %) was transferred to two selected liquid media and incubated under stationary conditions at 28 °C for a defined time period (usually 12-15 d) for the production of the BNM with the desired thickness (1 cm). BNM was rinsed thoroughly with distilled water and treated with 0.3 M NaOH solution in an autoclave (Hirayama, Japan) at 121 °C for 20 min to eliminate any remnants of bacterial colonies. The BNM was again thoroughly rinsed with distilled water till reaching neutral pH and stored at 4 °C for further use [4, 7, 8].

Preparation and evaluation of RAN loading and entrapment efficiency of BNM

The BNM was fabricated with the help of a locally designed circular-shaped disc fabricator (1.5 cm diameter) [8]. After partial removal of the water, the BNMs with the diameter 1.5 cm and thickness 1 cm created from culture media (SM, CW) were added a RAN solution by using absorption method in the optimized conditions (drug concentration: 250 mg/ml; temperature: 50 °C; shaking speed: 140 rpm; time of drug absorption: 150 min). The concentration of the RAN remaining in the loading solution was determined using a UV-Vis spectrophotometer (UV-Vis 2450, Shimadzu, Japan) at 314 nm [18]. A calibration curve of RAN solution in HCl 0.1N within the concentration range of 1 μg/ml to 6 μg/ml was used for determining RAN loadings in BNMs samples. The amount of loaded RAN into BNM was calculated according to formula 1 [3, 6, 22].

$$mab = (m1 - m2) \ (1)$$

Where mab is the amount of RAN that is loaded into the BNM (actual amount of drug); m1 is the initial RAN dose in solution (theoretical amount of drug); m2 is the excessive amount of RAN existing in the solution after a certain period of time BNM absorbs the RAN. The RAN entrapment efficiency (EE) of BNMs was calculated according to formula 2.

$$EE \ (\%) = \frac{mab}{m1} x100\% \ (2)$$

Morphological analysis

The surface topography and morphology of the BNMs and BNMs-RAN were visualized by a field emission scanning electron microscopy (FESEM, S-4800, Hitachi, Japan). The samples heat at 40 °C in 20 min, cover, then a thin platinum layer and put into the sample chamber [3, 4, 8, 10].

Fourier transform infrared spectroscopy analysis

Fourier transform infrared (FTIR) analysis was performed to characterize the presence of specific chemical groups to confirm the presence of RAN in BNMs using FTIR Affinity-1S (Shimadru, Japan). Spectra for all samples is directly measured by Reflectometry in 20 °C, moisture 40-43 %. The samples were scanned in the IR range from 400 to 4000 cm^{-1} [14, 19]. Interaction between the components, if any, was indicated by either producing additional peaks or absence of characteristic peak corresponding to RAN and BNMs.

Swelling behavior analysis

To study the swelling behavior of BNMs-RAN, the swelling degree (amount of water uptake) was measured by immersion of the known weight dried samples in test tubes, including 30 ml simulated gastrointestinal fluid (SGF, pH 1.2; and SIF, pH 6.8) at 37 °C for 24 h. Then, the water on the surfaces of the samples should be eliminated with filter paper and the specimens are to be weighed in wet condition. The swelling ratio (SR) of test samples was measured based on the formula 3 [10, 19, 22].

$$SR \ (\%) = \frac{(Mw-Md)}{Mw} x100\% \ (3)$$

Where Md is the weight of dried sample and Mw is the weight of swollen sample.

In vitro RAN release analysis

The *in vitro* RAN release analysis from BNMs-RAN (BNM-SM-RAN, BNM-CW-RAN) and RAN tablets were performed in simulated gastrointestinal fluid (SGF, pH 1.2; and SIF, pH 6.8) for 24 h [19]. The dissolution test apparatus fixed with eight rotating paddles (Agilent 708-DS Dissolution Apparatus, Malaysia) was used. Test samples (BNM-SM-RAN, BNM-CW-RAN and RAN tablets) were placed in 900 ml of the same SGF or SIF medium and kept at 37±0.1 °C under a stirring rate of 50 rpm. At known time intervals (0, 0.5, 1, 2, 4, 6, 8, 12, and 24 h), 5 ml aliquots of the solution were withdrawn from the release medium and replaced with the fresh solution to keep the total volume 900 ml. The withdrawn solution was applied to determine the RAN of release medium using a UV-Vis spectrophotometer (UV-Vis 2450, Shimadzu, Japan) at the wavelength of 315 nm for buffer solution with pH 1.2; 314 nm for buffer solution with pH 6.8. A calibration curve for RAN was plotted against its concentration in buffer solutions (pH 1.2, 6.8) within the concentration range of 1 μg/ml to 6 μg/ml and was regressed into linear line corresponding to the regression equation: y = 0.0047x+0.0298 (R^2 = 0.9998) for pH 1.2 and y = 0.0045x+0.0473 (R^2 = 0.9997) for pH 6.8 (where y is the absorbance of the RAN solution and x is the concentration of the RAN). The cumulative release ratio (CR) of RAN from the samples was calculated based on the formula 4 [22].

$$CR \ (\%) = \frac{C_t x V_1 + \sum_{i=1}^{i=n-1} C_i x V_2}{m} x100\% \ (4)$$

Where C$_t$ is the concentration of RAN in the buffer solutions at t time, V$_1$ is the volume of buffer solution at different pH values (900 ml, and pH 1.2, 6.8), n is the number of samples removed from the release medium, V$_2$ = 5 ml, and m is the initial total amount of RAN in the samples.

Kinetics and mechanism of drug release

In vitro drug release data were analyzed by using different kinetic models to find the mechanism of drug release. The values of various kinetic models were calculated with the help of DDSolver, an add-in extension for Microsoft Excel [24]. The mechanism of RAN release from the BNMs-RAN was calculated by fitting release data with different release kinetic models such as zero order, first order, Higuchi's and Korsmeyer-Peppas equations. Data of release kinetics, such as of kinetic rate constant (k), correlation coefficient (R^2) and release exponent (n) were calculated for the determination of the best fit model [4, 7, 11, 13, 16].

Data analysis and statistics

All the results obtained in the above-mentioned experiments are stated as mean±SD (Standard deviation) and are shown in the fig. and tables. The difference between the groups was evaluated by the one-way ANOVA test, using the Analysis ToolPak in Microsoft Excel 2010 and DDSolver (an add-in extension for Microsoft Excel) [24]. The differences are considered to be statistically significant when the P values are less than 0.05. All experiments were repeated at least three times.

RESULTS AND DISCUSSION

Preparation of BNMs and BNMs-RAN

Regarding cost-effective BNM for bio-phamercutical applications, the BNM in the present study produced by *K. xylinus* was compared in a low-cost substrate medium (CW) and a standard medium (SM). After the activated bacteria, *K. xylinus* was cultured in the nutrient media (SM, CW) [9] from 12 to 15 d at 28 °C for producing BNM with the desired thickness (1 cm). The results showed that the time for producing BNM with a thickness of 1 cm was longer in CW (15 d)

than in SM (12 d) under the same conditions. Therefore, SM is a better medium than CW for BNM production. However, the SM is expensive due to yeast extract used as a key nitrogen source. In this work, BNM was successfully produced by *K. xylinus* from both fermentative media containing SM and CW under static conditions. The BNMs with a diameter of 1.5 cm and a thickness of 1 cm (similar to the size of the commercially available RAN tablets) were fabricated with the help of a locally designed circular-shaped disc fabricator (1.5 cm diameter) [8]. After partial removal of the water, the BNMs produced from selected media (SM, CW) were added a RAN solution by using absorption method in the optimized conditions (drug concentration: 250 mg/ml; temperature: 50 °C; shaking speed: 140 rpm; time of drug absorption: 150 min). At the end of the experiment, the sample was removed from the absorbent solution to measure the OD (optical density), based on the RAN's calibration curve to calculate the amount of loaded RAN and the RAN entrapment efficiency of the BNMs. The results in table 1 showed that there was a significant difference in the amount of loaded RAN (mg) or RAN entrapment efficacy (%) of BNMs, which were produced from different culture media (SM, CW). The BNM-CW showed higher drug loading and entrapment efficiency, probably due to the difference of the density and porous fibrous network of BNM produced in selected media (SM, CW), facilitating the diffusion of the drug into BNM [4, 8].

Characterization of BNMs and BNMs-RAN

BNM is a nanofibrillar form of cellulose with a porous structure and high water-holding capacity. The swelling behavior would possibly represent the relative evaluation of the entanglement and the compression between the nanofibers [19]. The swelling ratio of BNMs-RAN was evaluated in the simulated gastrointestinal conditions (SGF, pH 1.2; and SIF, pH 6.8). The results of the swelling profile of BNMs-RAN are shown in table 2.

Table 1: Evaluation of RAN loading and entrapment efficiency of BNMs (All values are expressed as mean±SD, n = 3)

BNM types	RAN loading (mg)	Entrapment efficiency (%)
BNM-SM	152.33±4.04	60.93±1.62
BNM-CW	167.00±4.58	66.80±1.83

Table 2: Evaluation of the swelling profile of BNMs-RAN in SGF or SIF at 37 °C (All values are expressed as mean±SD, n = 3)

Formulations	SGF (pH 1.2) (%)	SIF (pH 6.8) (%)
BNM-SM-RAN	74.67±2.52	60.33±3.21
BNM-CW-RAN	90.67±3.06	81.00±2.65

As listed in table 2, the swelling behavior results show that this parameter of BNMs-RAN occurring at pH 1.2 is higher than in pH 6.8 medium. The result of the present study is also supported by those of a previous study in which indicating fiber expansion of BNM in treatment with acid [4]. While the BNM-SM-RAN can absorb 74.67±2.52 % of the water in SGF or 60.33±3.21 % of the water in SIF, BNM-CW-RAN has a water uptake capacity of 90.67±3.06 % in SGF or 81.00±2.65 in SIF. These values demonstrate that the low density and high porous fibrous network of BNM-CW consequence the raise of the distance between these nanofibers, and the increased penetration of water into nanofibers.

The nanoscale fibril network of BNM produced by *K. xylinus* in SM and CW was visualized under FESEM. The FESEM images in fig. 1 showed that the randomly oriented and densely packed network of ultrafine fibrils was observed in the BNM synthesized by *K. xylinus* in SM and CW. As a result, FESEM images of the cross-section and surface view of BNM showed a clear, well organized, densely arranged and interconnected porous nanofibrous network. The results are in agreement with the previous studies [3, 4, 7, 8].

It is clearly observed that FESEM analysis of cross-sections of the RAN-loaded BNM in comparison with an unloaded BNM sample showed that the structure of samples was not affected throughout the different processes in terms of the fiber network. A tendency of an increase in the size of pore areas due to further swelling processes during the loading procedure could be observed. BNM-SM showed slightly higher fiber diameters and lower pore sizes than BNM-CW, probably caused by a decrease in fiber distances and partial assembly of adjacent polymer fibers.

FTIR spectra of RAN, BNM-SM, BNM-CW, BNM-SM-RAN, and BNM-CW-RAN were recorded and are presented in the fig. 2, 3, 4, 5, and 6. The study of the FTIR spectra of RAN has shown in fig. 2 demonstrated that a band at 3504 cm^{-1} connected to the overlapped stretching vibrations of OH and NH_2 functional groups. The absorption peaks appeared at 2938, 1633 and 1408 cm^{-1} were imputed to the C-H stretching, amide bending and $-CH_2$ bending vibrations, respectively [19]. The FTIR spectra of BNM in this study displayed the typical features of cellulosic substrates with intense bands around 3341, 2894, 1107 and 612 cm^{-1}, associated with the vibrations of the -OH, C-H, C-O-C and $-CH_2$- groups, respectively [4, 17].

The obtained data revealed that in the RAN loaded BNM, no additional peaks attributable to the formation of a complex appeared, but variations in the relative intensities of the characteristic peaks for BNM and the RAN can be observed. It has been observed that the absorption bands of both RAN and RAN with BNMs remaining the same. It was concluded that no such interaction between the RAN and BNMs was occurring. Moreover, the appearance of specific absorption peaks associated with functional groups of BNM and RAN (fig. 5 and 6) revealed the successful RAN loading into BNM without any chemical alteration in the structure of the RAN and BNM.

Evaluation of *in vitro* drug release

The release profiles of RAN from the commercial tablets containing RAN (TAB-RAN), BNM-SM-RAN and BNM-CW-RAN were investigated in the simulated gastrointestinal conditions (SGF, pH 1.2 and SIF, pH 6.8), and obtained results are shown in fig. 7 and fig. 8.

A

B

C

D

E

F

G

H
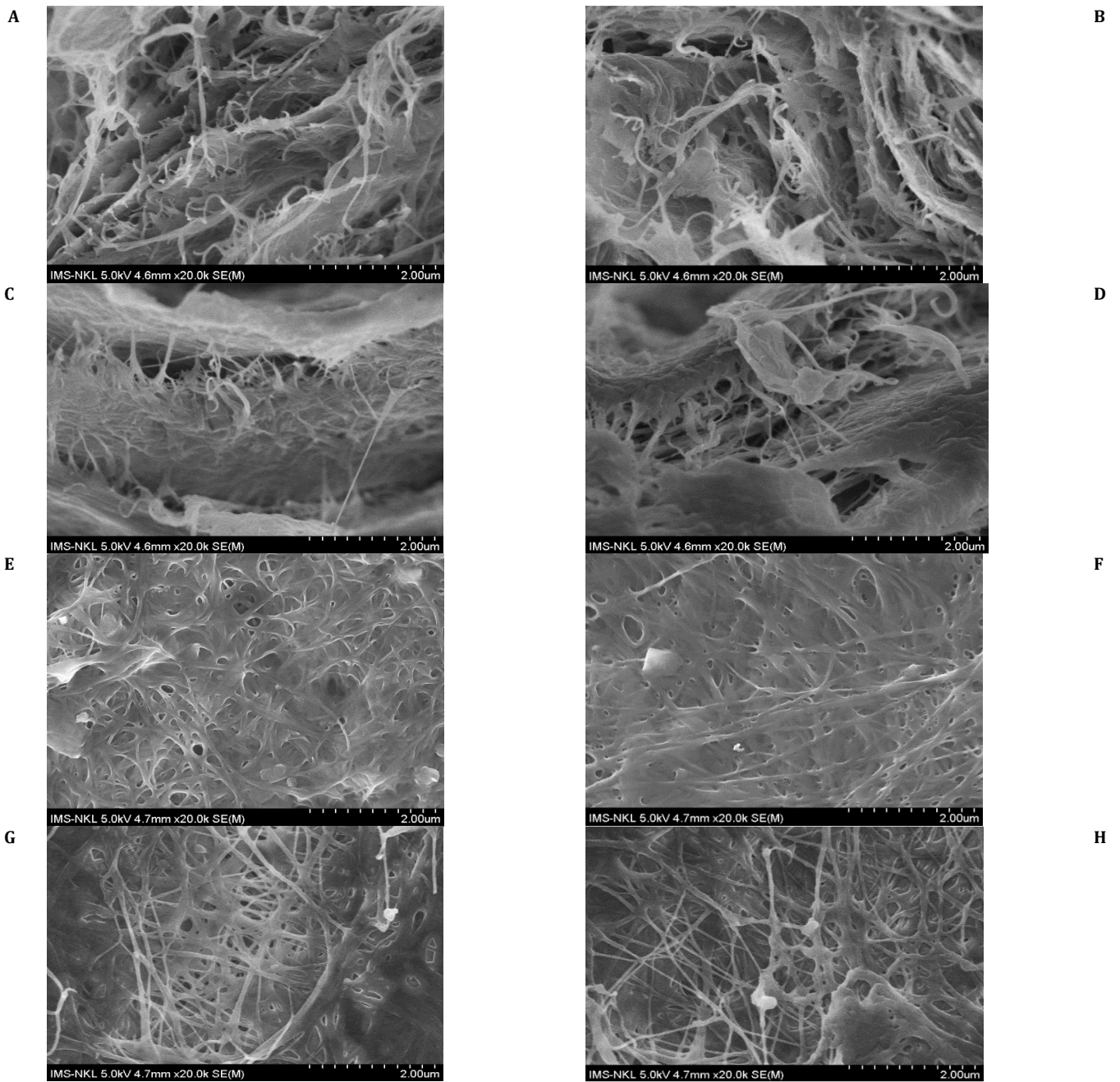
Fig. 1: Morphological characterization of BNMs and BNMs-RAN. FESEM images of BNM-SM on cross-section view (A) and surface view (E), BNM-SM-RAN on cross-section view (B) and surface view (F), BNM-CW on cross-section view (C) and surface view (G), BNM-CW-RAN on cross-section view (D) and surface view (H)
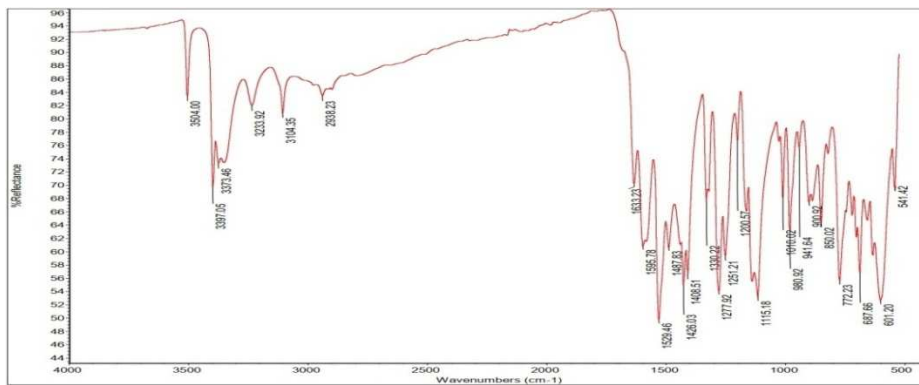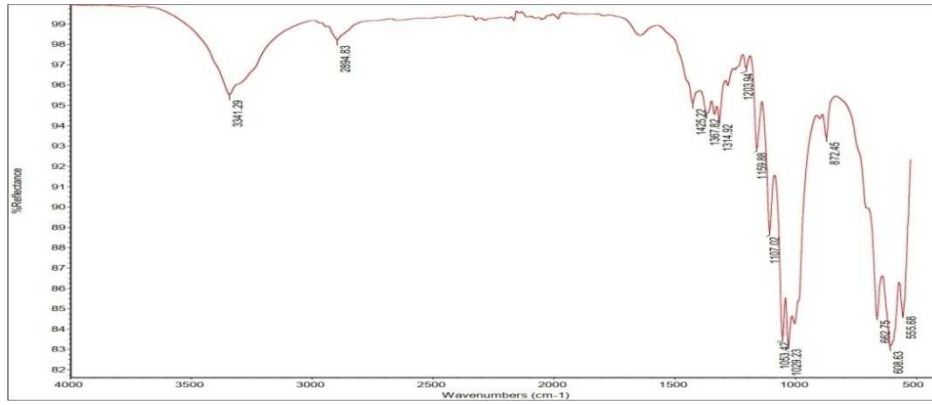
Fig. 2: FTIR spectra for ranitidine (RAN)
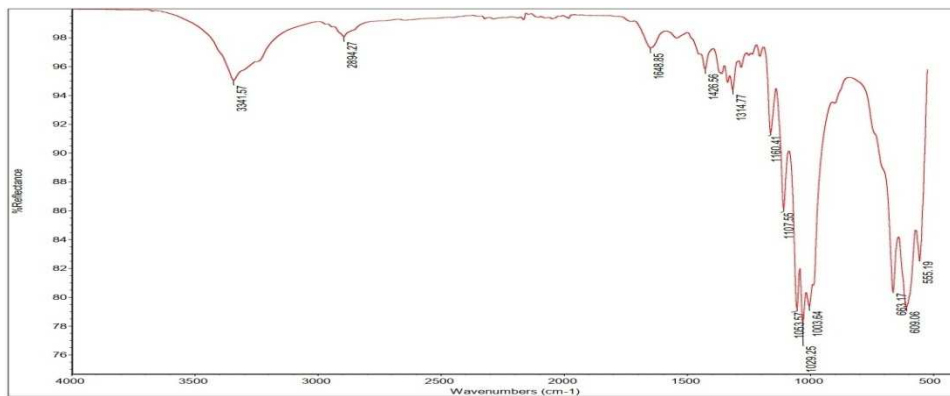
Fig. 3: FTIR spectra for BNM-SM
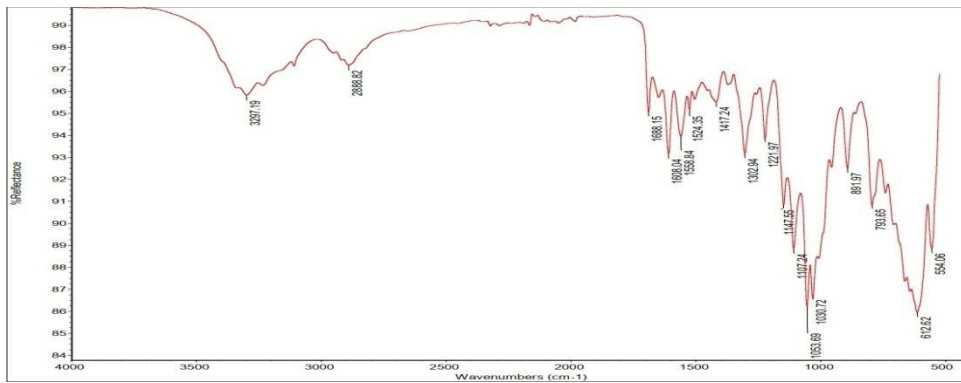

Fig. 4: FTIR spectra for BNM-CW

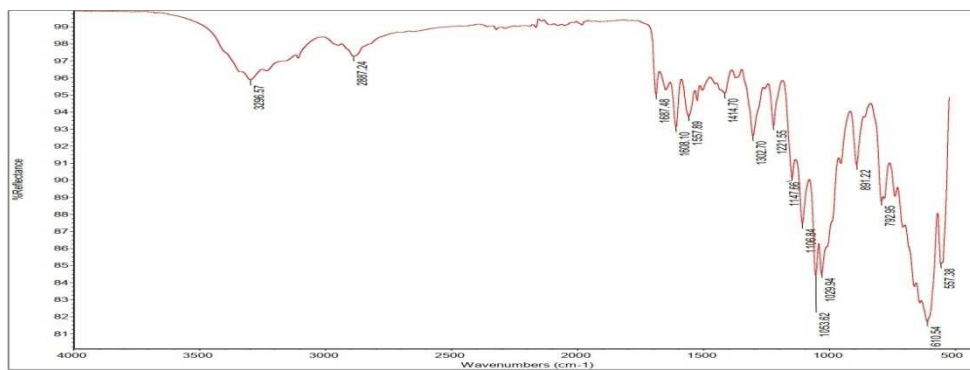**Fig. 5: FTIR spectra for BNM-SM-RAN**

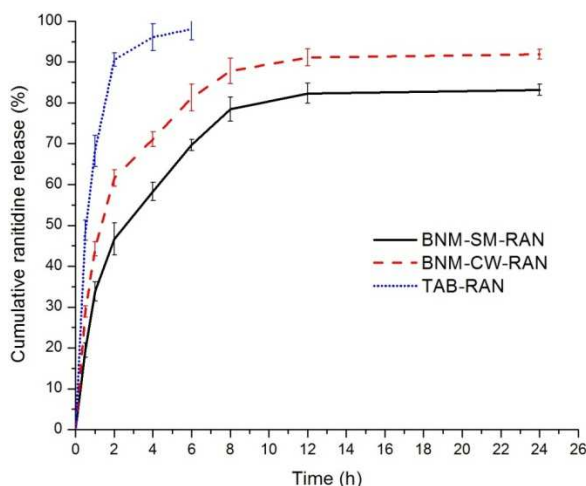**Fig. 6: FTIR spectra for BNM-CW-RAN**

Fig. 7: *In vitro* RAN release profiles for BNMs-RAN and TAB-RAN in SGF at 37 °C (Results are expressed as mean±SD, n=3)
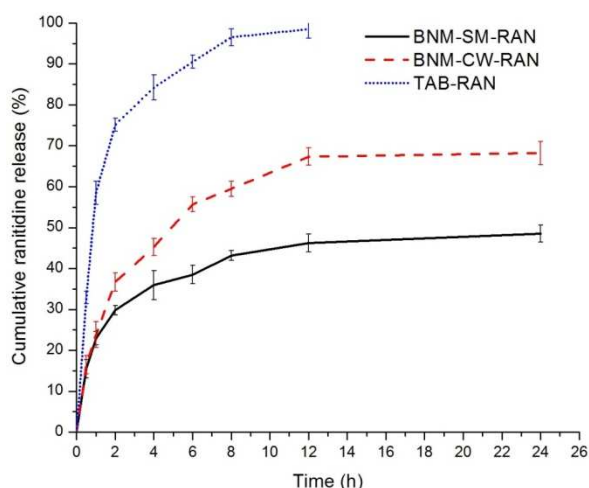

Fig. 8: *In vitro* RAN release profiles for BNMs-RAN and TAB-RAN in SIF at 37 °C (Results are expressed as mean±SD, n=3)

As it could be observed from fig. 7 and fig. 8, the commercial tablets containing RAN (TAB-RAN) in the simulated gastrointestinal conditions exhibited a burst RAN released in a short time period because of the rapid dissolution of RAN in the simulated gastric conditions [19]. The *in vitro* release profiles in all experimental simulated gastrointestinal conditions showed a significant difference (P<0.05) in the release of RAN from BNMs-RAN, suggesting pH-dependent release. However, the TAB-RAN showed a distinct release pattern when compared to the release of RAN from BNMs-RAN. More than 90% of the RAN was released from the TAB-RAN in the first 2-4 h of study at all two simulated pH media. As a result, most of the drug will reach the blood for systemic action after absorption through the gastrointestinal tract that may lead to fluctuations in plasma drug levels and undesirable side effects. However, a high initial burst RAN release from the BNMs-RAN could not be seen in the initial hours. A key reason for the sustained drug release might have imputed to the 3D weblike nanofibrous network structure of BNM, which limited the movability the nanofibers, resulted in the reduction of the initial burst RAN release from BNMs-RAN. As the results showed in fig. 7 and fig. 8, the content and the rate of RAN released from the BNMs-RAN at pH 6.8 are lower than those at pH 1.2. BNM had a pH-responsive feature that has been demonstrated in a previous study [4]. The higher swelling ratio was attained when the entrance of the swelling fluid into the nanofibers was facilitated. The more the nanofibers swell, the more the fluid diffuse within the nanofibers and the more the trapped drug would be released [19].

Moreover, the RAN release from BNM-SM-RAN in both SGF and SIF

medium was found slower from BNM-CW-RAN. The nanofiber density and extremely porous network of BNM-CW could be the possible reason for the faster RAN release. Swelling behavior studies and FESEM analysis confirm this hypothesis.

Kinetics and mechanism of drug release

Drug release profiles of the BNMs-RAN and TAB-RAN were fitted into zero-order, first-order, Higuchi's and Korsmeyer-Peppas models to describe the kinetic behavior of the drug release mechanism from the formulations, the most suitable being the one that best fits the experimental results. The correlation coefficients for the different drug release kinetic models are shown in tables 3 and 4. In both SGF and SIF medium, the BNM-SM-RAN and BNM-CW-RAN followed Korsmeyer-Peppas kinetics with high linearity, whereas the TAB-RAN followed first-order kinetics. To confirm the diffusion mechanism, the data were fitted into the Korsmeyer-Peppas model. The use of Korsmeyer-Peppas equation, the interpretation of release exponent (n) values, gives an insight into the release mechanisms. According to the Korsmeyer-Peppas model, an amount of n<0.5/0.45/0.43 for a slab/cylinder/sphere indicates a diffusion controlled drug release process [4, 13]. As the results showed in tables 3 and 4, all the n values were less than 0.5, so Fickian diffusion is the predominant drug release mechanism. These findings are in agreement with previous studies reported in the literature, whereby drug release follows Ritger-Peppas kinetics from through the polymeric porous three-dimensional matrix [4].

Table 3: Values of correlation coefficient (R^2), the kinetic rate constant (k), and release exponent (n) from BNMs-RAN and TAB-RAN in SGF at 37 °C

Formulations	Zero-order		First-order		Higuchi		Korsmeyer-Peppas		
	R^2	k	R^2	k	R^2	k	R^2	k	n
BNM-SM-RAN	0.2436	5.23	0.8861	0.23	0.7579	22.88	0.9381	37.67	0.29
BNM-CW-RAN	0.6666	5.88	0.9197	0.41	0.6059	26.21	0.9435	48.63	0.24
TAB-RAN	0.7795	21.77	0.9988	1.21	0.9278	49.13	0.9843	67.28	0.24

Table 4: Values of correlation coefficient (R^2), the kinetic rate constant (k), and release exponent (n) from BNMs-RAN and TAB-RAN in SIF at 37 °C

Formulations	Zero-order		First-order		Higuchi		Korsmeyer-Peppas		
	R^2	k	R^2	k	R^2	k	R^2	k	n
BNM-SM-RAN	0.5613	3.01	0.8474	0.08	0.6654	13.25	0.9703	24.04	0.25
BNM-CW-RAN	0.1180	4.21	0.7079	0.12	0.8073	18.26	0.9501	28.84	0.31
TAB-RAN	0.7893	11.53	0.9718	0.73	0.7633	35.59	0.9592	55.60	0.26

Although the release rate for RAN from BNM-SM-RAN was slower than for RAN from BNM-CW-RAN in both SGF and SIF medium, the drug release mechanism was the same.

CONCLUSION

Oral sustained-release RAN delivery system based on BNMs was successfully developed and evaluated for various *in vitro* parameters. The amount of loaded RAN or entrapment efficacy for BNM-CW is higher than for BNM-SM. The BNM-SM-RAN and BNM-CW-RAN exhibited a decreased initial burst release system followed by a prolonged RAN release up to 24 h in relation to the commercial tablets containing RAN. The RAN release from these formulations was found higher in the SGF medium than that of in SIF medium. RAN released from these formulations was found to follow the Korsmeyer-Peppas model and diffusion sustained drug release mechanism. The sustained release of RAN from BNM-SM-RAN was slower than for RAN from BNM-CW-RAN, but the mechanism of sustained RAN release was the same. Based on the obtained results, the biopolymers like BNM-SM and BNM-CW could be utilized to develop oral sustained RAN release dosage form.

AUTHORS CONTRIBUTIONS

The authors declare that this work was done by the authors named in this article and all liabilities pertaining to claims relating to the content of this article will be borne by them.

CONFLICT OF INTERESTS

The authors declare that there are no conflicts of interest.

REFERENCES

1. Sharma C, Bhardwaj NK. Bacterial nanocellulose: present status, biomedical applications and future perspectives. Mater Sci Eng Carbon 2019;104:1-18.
2. Potzinger Y, Kralisch D, Fischer D. Bacterial nanocellulose: the future of controlled drug delivery. Ther Delivery 2017;8:753-61.
3. Muller A, Ni Z, Hessler N, Wesarg F, Muller FA, Kralisch D, *et al.* The biopolymer bacterial nanocellulose as drug delivery system: an investigation of drug loading and release using the model protein albumin. J Pharm Sci 2013;102:579-92.
4. Huang L, Chen X, Nguyen TX, Tang H, Zhang L, Yang G. Nano-cellulose 3D-networks as controlled-release drug carriers. J Mater Chem B 2013;1:2976-84.
5. Moritz S, Wiegand C, Wesarg F, Hessler N, Muller FA, Kralisch D, *et al.* Active wound dressings based on bacterial nanocellulose as drug delivery system for octenidine. Int J Pharm 2014;471:45-55.
6. Wiegand C, Moritz S, Hessler N, Kralisch D, Wesarg F, Muller FA, *et al.* Antimicrobial functionalization of bacterial nanocellulose by loading with polihexanide and povidone-iodine. J Mater Sci Mater Med 2015;26:1-14.
7. Ullah H, Badshah M, Makila E, Salonen J, Shahbazi MA, Santos HA, *et al.* Fabrication, characterization and evaluation of bacterial cellulose-based capsule shells for oral drug delivery. Cellulose 2017;24:1445-54.
8. Badshah M, Ullah H, Khan SA, Park JK, Khan T. Preparation, characterization and *in vitro* evaluation of bacterial cellulose matrices for oral drug delivery. Cellulose 2017;24:5041-52.
9. Subtaweesin C, Woraharn W, Taokaew S, Chiaoprakobkij N, Sereemaspun A, Phisalaphong M. Characteristics of curcumin-loaded bacterial cellulose films and anticancer properties against malignant melanoma skin cancer cells. Appl Sci 2018;8:1-15.
10. Morais ES, Silva NHCS, Sintra TE, Santos SAO, Neves BM, Almeida IF, *et al.* Anti-inflammatory and antioxidant nanostructured cellulose membranes loaded with phenolic-based ionic liquids for cutaneous application. Carbohydr Polym 2019;206:187-97.
11. Marabathuni VJ, Deveswaran R, Bharath S, Basavaraj BV, Madhavan BV. Design and optimization of multiparticulate gastroretentive delivery system of ranitidine hydrochloride. Int J Pharm Pharm Sci 2012;4:597-603.
12. Patel R, Bathe RS, Khobragade D, Jadhav S. Formulation and evaluation of gastroretentive beads of ranitidine hydrochloride. Int J Pharm Pharm Sci 2014;6:237-42.
13. Maharjan R, Subedi G. Formulation and evaluation of floating in situ gel of ranitidine using natural polymers. Int J Pharm Pharm Sci 2014;6:205-9.
14. Dixit GR, Chavhan JI, Upadhye KP, Misra S. Formulation and characterization of the mucoadhesive buccal film of ranitidine hydrochloride using sterculia Foetida gum as polymer. Asian J Pharm Clin Res 2015;8:68-71.
15. Etman ME, Mahmoud EH, Galal S, Nada AH. Floating ranitidine micro particulates: development and *in vitro* evaluation. Int J Appl Pharm 2016;8:1-9.
16. Rajeswari S, Kudamala S, Murthy KVR. Development, formulation, and evaluation of bilayer gastric retentive floating tablets of ranitidine HCl and clarithromycin using natural polymers. Int J Pharm Pharm Sci 2017;9:164-77.
17. Sahu VK, Sharma N, Sahu PK, Saraf SA. Formulation and evaluation of floating-mucoadhesive microspheres of novel natural polysaccharide for site-specific delivery of ranitidine hydrochloride. Int J Appl Pharm 2017;9:15-9.
18. Maraie NK, Salman ZD, Yousif NZ. Design and characterization of oroslippery buoyant tablets for ranitidine hydrochloride. Asian J Pharm Clin Res 2018;11:143-9.

19. Darbasizadeh B, Motasadizadeh H, Foroughi-Nia B, Farhadnejad H. Tripolyphosphate-crosslinked chitosan/poly (ethylene oxide) electrospun nanofibrous mats as a floating gastro-retentive delivery system for ranitidine hydrochloride. J Pharm Biomed Anal 2018;153:63-75.
20. Torne SR, Sheela A, Sarada NC. Ranitidine controlled release anti-reflux suspension for gastro-oesophageal reflux disease and it's *in vitro* evaluation. Int J Appl Pharm 2019;11:74-81.
21. Jafar M, Mohsin AA, Khalid MS, Alshahrani AM, Alkhateeb FS, Alqarni AS. Ranitidine hydrochloride stomach specific bouyant microsponge: Preparation, *in vitro* characterization, and *in vivo* anti-ulcer activity. J Drug Delivery Sci Technol 2020;55:1-8.
22. Xu J, Tan X, Chen L, Li X, Xie F. Starch/microcrystalline cellulose hybrid gels as gastric-floating drug delivery systems. Carbohydr Polym 2019;215:151-9.
23. Hestrin S, Schramm M. Synthesis of cellulose by *Acetobacter xylinum*, 2. Preparation of freeze-dried cells capable of polymerizing glucose to cellulose. Biochem J 1954;58:345-52.
24. Zhang Y, Huo M, Zhou J, Zou A, Li W, Yao C, *et al.* DDSolver: an add-in program for modeling and comparison of drug dissolution profiles. AAPS J 2010;12:263-71.